RSC Advances

PAPER

View Article Online
View Journal | View Issue

Cite this: *RSC Adv.*, 2017, **7**, 6358

Tunable metal-enhanced fluorescence by pH-responsive polyacryloyl hydrazide capped Ag nanoparticles†

Shuai Yuan,[a] Fengyan Ge,*[ab] Yanmin Chen[a] and Zaisheng Cai[a]

Received 23rd November 2016
Accepted 4th January 2017

DOI: 10.1039/c6ra27193f

www.rsc.org/advances

A new strategy for metal enhanced fluorescence (MEF) was firstly realized based on the surface plasmon resonance of polyacryloyl hydrazide capped Ag nanoparticles (PAH–Ag NPs). Owing to the pH-responsive swelling–shrinking behavior of the polyacryloyl hydrazide (PAH) polymer, the interaction distance between the Por^{4+} dye molecules and Ag NPs can be controlled under pH stimuli. By this method, we successfully achieved a tunable MEF in the pH range from 4 to 9 and 1.97-fold fluorescence enhancement can be obtained at pH = 4 as compared to the reference. The as-prepared PAH–Ag NPs successfully combined pH sensitivity and the controllable MEF effect into one entity by introducing the PAH polymer on the surface of Ag NPs, which is promising for use as materials for selective biological sensing and imaging.

Introduction

In recent years, the fluorescence technique has attracted much attention because of its simplicity and sensitivity in the fields of chemistry, biochemistry and sensing devices.[1–6] However, in some cases, some biomolecules cannot be effectively detected by fluorescence analysis owing to the presence of endogenous fluorescers.[7] To overcome this limitation, considerable efforts have been devoted to improving the sensitivity of fluorescence measurements. The successful strategies, such as photonic crystals (PCs) enhanced fluorescence, fluorescence resonance energy transfer (FRET) enhanced fluorescence and metal enhanced fluorescence (MEF), have been demonstrated to amplify the fluorescence signals.[8–13] Among these methods, MEF shows great potential for the detection and imaging of biological species such as DNA, RNA and proteins.

The MEF effect is a unique phenomenon whereby when a fluorophore is in close proximity to the nanostructures of noble metals (silver, gold), the fluorescence intensity and stability of fluorophores can be greatly increased. This phenomenon is attributed to coupling of the oscillating dipole of the fluorophore with the plasmon resonance from the surface of the metal.[14,15] In these reports of MEF, Ag nanoparticles (Ag NPs) are most commonly employed for easy preparation and excellent surface plasmon resonance. When the fluorophore is close to the surface of the Ag NPs, strong electromagnetic fields will be generated, resulting in the fluorescence intensity enhancement of fluorophores.[16,17] MEF is sensitive to the interaction distance between the fluorophores and the Ag NPs. If the distance between fluorophores and the surface of the Ag NPs is too close, the existence of Ag NPs will have a pronounced tendency to quench the fluorescence. In contrast, there is no interaction to perform MEF effects. Therefore, MEF can be controlled by adjusting the distance between the fluorophores and Ag NPs.[18,19]

The introduction of the stimuli responsive polymers on the surface of Ag NPs has been proved to be an effective approach to control the MEF.[20,21] The swelling–shrinking behavior of the responsive polymer can control the distance between the Ag NPs and the fluorophore with an appropriate external stimuli (such as temperature and pH) and further achieve the tunable MEF effects.[22,23] As a pH-responsive polymer, polyacryloyl hydrazide (PAH) has already been reported for various biomedical applications.[24,25] Owing to abundant hydrazide functionality, PAH can not only serve as the reducing agent for the metal ion precursors, but can also swiftly encapsulate the surface and stabilize the metal NPs.[26] PAH was used as a nanoreactor to synthesize Ag NPs and at the same time Ag NPs were dispersed in the stimuli nanoparticles. Therefore, we employed tunable MEF effects by adjusting the interaction distance between the fluorophores and the Ag NPs owing to the pH responsive swollen–shrunken state of PAH under pH stimuli.

In this paper, pH-responsive PAH–Ag NPs were prepared by a simple synthesis method without adding a reducing agent. PAH–Ag NPs were used to adsorb positively charged Por^{4+} dyes onto the surfaces of PAH–Ag NPs. As shown in Scheme 1, owing

[a]College of Chemistry, Chemical Engineering and Biotechnology, Donghua University, Shanghai 201620, People's Republic of China. E-mail: fyge@dhu.edu.com; Tel: +86-21-67792608-804

[b]Key Laboratory of Textile Science & Technology (Donghua University), Ministry of Education, China

† Electronic supplementary information (ESI) available. See DOI: 10.1039/c6ra27193f

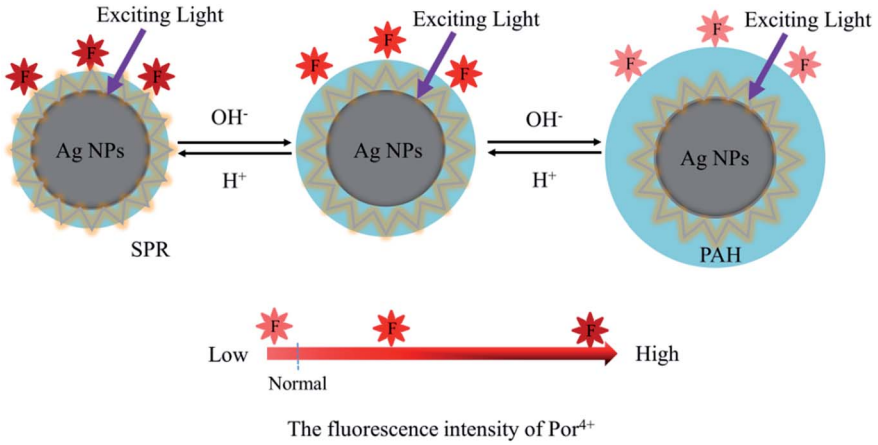

Scheme 1 Schematic illustration of the tunable MEF effects of Por^{4+} with PAH–Ag NP by adjusting the pH.

to the responsiveness of PAH polymer, the distance between the Ag NPs and the Por^{4+} fluorescence can be easily controlled by different pH values. Correspondingly, a tunable MEF effect of the Por^{4+}/PAH–Ag NPs can be realized by adjusting the pH.

Experimental

Materials

5,10,15,20-Tetrakis-(*N*-methyl-4-pyridyl)-21,23*H*-porphyrin tetratosylate (Por^{4+}) and tetrabutyl ammonium bromide (TBAB) were purchased from Sigma-Aldrich. Other chemicals and solvents were purchased from Shanghai Chemical Reagent Co and were used without further purification. Deionized water was used in the process of synthesis and characterization.

Instrumentation

Transmission electron microscopy (TEM) images of the PAH–Ag NPs were obtained using a 2100F transmission electron microscope (JEOL, Japan) at a voltage of 200 kV and the diluted PAH–Ag NPs dispersions were dropped onto carbon coated copper grids and dried before observation. The hydrodynamic diameters (D_h) of the PAH–Ag NPs at the various pH values were detected *via* BI-200SM dynamic light scattering (DLS) with a BI-9000 AT digital time correlator (Brookhaven, USA) in the condition of 90° for scattering angle. Laser source is a He–Ne laser with 633 nm and 35 mV. The ζ potentials of the PAH–Ag NPs dispersed in the waters at various pH values were measured *via* a Nano-ZS (Malvern, UK) using a monochromatic coherent He–Ne laser as the light source. The UV-visible spectra of PAH–Ag NPs dispersed in the waters at various pH values were tested *via* a UV-visible spectrometer (PerkinElmer, USA). The fluorescence spectra of the PAH–Ag NPs were measured using a Hitachi F-7000 spectrofluorometer with pH stimuli.

Preparation of PAH

PAH was synthesized using a procedure reported earlier.[27] Polymethyl acrylate (PMA) was prepared according to Moustafa report.[28] Then PMA (0.156 mol) were dissolved in 300 mL tetrahydrofuran, hydrazine hydrate (0.8 mol) and TBAB (0.031 mol) were added to it. The mixed solution was heated to 60 °C and lastly reacted for 12 h. The prepared PAH solution was transferred into methanol to form the polymer product. The obtained white product was washed several times and dried at ambient temperature under reduced pressure for further use. Yield: 90%. ^{1}H NMR (400 MHz, D_2O) δ (ppm): 1.3–2.2 (m, 3H, $-CH_2-CH-CO-$), 3.16 (br, 2H, $-CONH-NH_2$).

Preparation of PAH–Ag NPs

PAH–Ag NPs were prepared without a reducing agent or modifier.[26] Briefly, 250 μL of $AgNO_3$ aqueous solution (0.05 mol L^{-1}) was added to 25 mL of PAH aqueous solution (2% (w/v)), then the mixture was stirred for 30 min at room temperature. The resulting reddish brown solution was purified by dialysis against deionized water for 24 h, collected by centrifugation, and then dispersed in deionized water.

Tunable MEF experiments

To study the tunable MEF effect of PAH–Ag NPs, the different pH values of the PAH–Ag solution were adjusted using 0.1 mol L^{-1} HCl solution. Then 20 μL of PAH–Ag NPs solution at different pH values was added to the Por^{4+} (10^{-6} M) solution and incubated for 2 h. The period of 2 h ensured sufficient adsorption of Por^{4+} to obtain veritable fluorescence intensities. Fluorescence measurements were performed using an excitation wavelength of 420 nm to determine the MEF effects. The MEF enhancement factors at various pH values were calculated by comparing the fluorescence intensity of the nanoparticle-added Por^{4+} solution at a wavelength of 653 nm and a pure Por^{4+} solution under the same measurement conditions.

Results and discussion

Synthesis and characterization of PAH–Ag NPs

PAH (M_n = 62 000 g mol^{-1}) with quantitative functionality can be conveniently synthesized (Fig. S1†). In this paper, we synthesized PAH by the treatment of PMA with hydrazine

hydrate as the reducing agent in the presence of TBAB as the catalyst, as shown in Scheme 2. The PAH possessed a hydrazide group in each repeating unit, which served as an effective reducing agent for the preparation of metal NPS in the chemical reduction of the metal ion in the polymeric matrixes, as reported in the literature.[29,30] Ag^+ electrophilic substitution of the nitrogen at the end of hydrazide groups formed –CO–NH–NH– and Ag NPs in the process of preparation of the PAH–Ag NPs. In addition, the presence of PAH on the surface of the Ag NPs can resist the oxidation of Ag^0 to Ag^+ and reduce the toxicity associated with Ag NPs.[26] We also confirmed the above-mentioned results through the experimental phenomena. When the solution of $AgNO_3$ was added into the PAH aqueous solution at ambient temperature, a characteristic yellow color of the reaction mixture appeared within 15 min, suggesting the formation of NPs. With the increase of the reaction time, the color of the solution became reddish brown, indicating the size increase of the Ag NPs. From Fig. 1a, the average size of the Ag NPs obtained was about 32 nm. As shown in Fig. 1b, we found that the Ag NPs were fully encapsulated by the PAH polymer with complete core–shell structures. From TG analysis (Fig. 2), we can calculate the content of the Ag NPs inside the PAH–Ag NPs to be 3.7% (w/w), which indicates that there were substantial organic constituents in the NPs, further illustrating the formation of PAH–Ag NPs. In addition, the FTIR spectra of PAH–Ag NPs (Fig. S2†) exhibited the characteristic bands at 1620 and 3253 cm^{-1} for $-C{=}O_{str}$ and $-N{-}H_{str}$, respectively, which also suggested that PAH was present on the surface of the Ag NPs.

In the PAH–Ag NPs, the Ag NPs showed a similar absorption peak (at about 407 nm) in UV-vis spectra in the pH range from 4 to 9 (Fig. 3). The imperceptible changes of the absorbance intensity and the location of the absorption peak were only attributed to the change of the thickness of the polymer shell layer. This indicated that the PAH did not obviously change the optical property of the Ag NPs in the nanoparticle during the swelling–shrinking process. Therefore, for the same size of Ag NPs, when the fluorophores were adsorbed on the surface of the PAH–Ag NPs, the MEF effects of PAH–Ag NPs can be mainly controlled by the distance between the metal and the fluorophore. By dynamic light scattering (DLS) (Fig. 4), we can find that the PAH–Ag NPs displayed obvious pH responsiveness owing to the presence of PAH on the Ag NPs surface. As

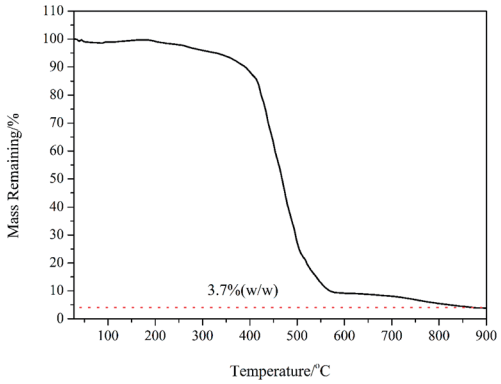

Fig. 2 Weight loss of PAH–Ag NPs as a function of temperature.

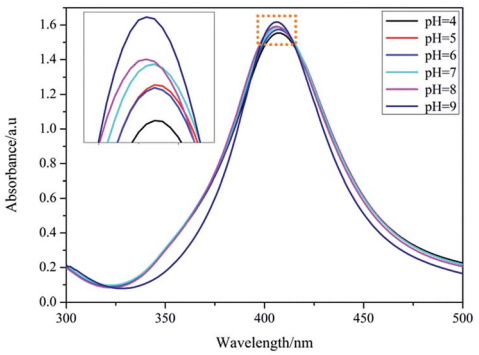

Fig. 3 pH dependence of the UV-vis absorption spectra of PAH–Ag NPs.

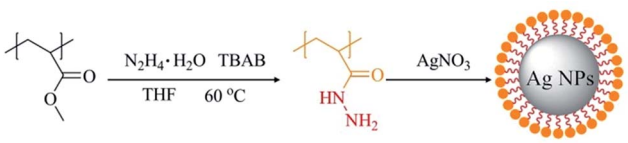

Scheme 2 Schematic illustration of the preparation of PAH–Ag NPs.

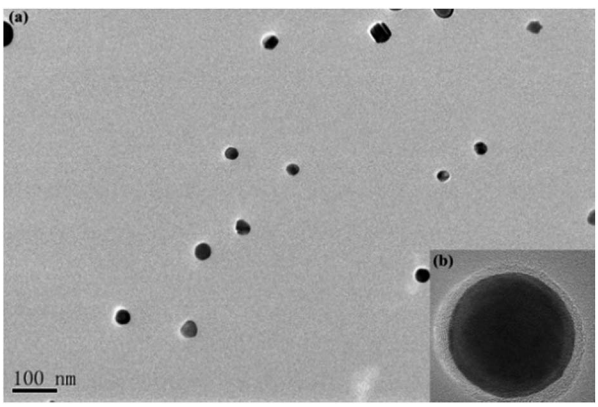

Fig. 1 (a) TEM images of PAH–Ag NPs; (b) HRTEM images of a single PAH–Ag NP.

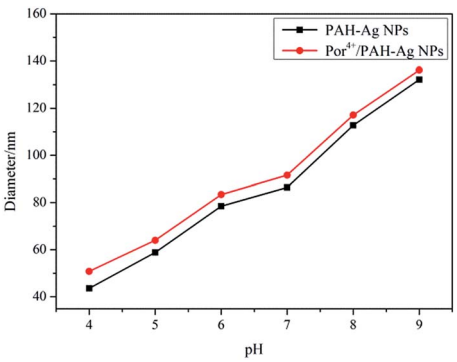

Fig. 4 pH dependence of the hydrodynamic diameter of PAH–Ag NPs and Por^{4+}/PAH–Ag NPs.

expected, the average diameters of the PAH–Ag NPs were changed by adjusting the pH. The hydrodynamic diameter of the PAH–Ag NPs was 132.2 nm at pH = 9 and decreased to 43.6 nm when the pH was 4. This could be attributed to the synergism effect of the following factors: protonation–deprotonation, charge repulsion and the hydrogen bond forming capacity of the PAH polymer. From Fig. 1a and 4, we can further calculate the thickness of the PAH by subtraction of the Ag NPs diameter from the diameter of the PAH–Ag NPs, which was 101.2 nm at pH = 9 and 11.6 nm at pH = 4. Owing to the MEF being sensitive to the interaction distance between the metal and the fluorophore, we studied the pH-responsiveness of the Por^{4+}/PAH–Ag NPs by DLS at various pH values (Fig. 4). As expected, the average diameters of the Por^{4+}/PAH–Ag NPs increased on increasing the pH, which was consistent with the swelling–shrinking property of the PAH–Ag NPs. The hydrodynamic diameter of the Por^{4+}/PAH–Ag NPs was measured as 136.2 nm at pH = 9 and collapsed to 50.8 nm when the pH was decreased to 4. The increase of the hydrodynamic diameter at the same pH could be attributed to the Por^{4+} layer adsorbed on the surface of the PAH–Ag NPs. In addition, we found that the increments of hydrodynamic diameter increased with the decrease of pH. This is because H^+ changed the ζ potential of the PAH–Ag NPs (see ESI, Fig. S3†), the attraction between the PAH–Ag NPs and Por^{4+} will weaken. Therefore, the increment of the hydrodynamic diameter increased at the decreased pH value.

Optical properties of PAH–Ag NPs

Por^{4+} is a positively charged fluorescent porphyrin derivative and its fluorescence property is very stable under different pH values, thus it is widely used as a fluorescent probe to detect MEF behavior.[31] Under the action of electrostatic attraction, a large number of Por^{4+} molecules were adsorbed on the surface of the PAH–Ag NPs, which was very useful for MEF. Therefore, we selected Por^{4+} as a fluorescent probe to detect the MEF behavior of the PAH–Ag NPs. By exploring the influence of incubation time on the PAH–Ag NPs enhanced Por^{4+} (Fig. 5), we found that if the incubation time exceeded 2 h, the fluorescence intensity of the Por^{4+} no longer increased and maintained a stable value, which indicated that a mass of Por^{4+} dye molecules were adsorbed on the surface of the PAH–Ag NPs. Therefore, we chose 2 h as the incubation time. In order to rule out the influence of the polymer PAH on the fluorescence intensity of Por^{4+}, the polymer of PAH and the bare Ag NPs (about 30 nm) with the same particle concentration as PAH–Ag were also used for the fluorescence experiments. From Fig. 6, we can see that the fluorescence spectra of Por^{4+} have not been significantly enhanced by introducing the pure polymer PAH. However, these results are different to those for the bare Ag NPs; the fluorescence emission of Por^{4+} reduced to about 43% of the original fluorescence intensity owing to adding Ag NPs.[32] In addition, the fluorescence intensity of Por^{4+} was obviously enhanced by the introduction of the PAH–Ag NPs. The above mentioned results fully confirmed that the pure polymer PAH disadvantaged the fluorescence enhancement and Ag NPs can quench the fluorescence of Por^{4+}. Importantly, owing to the presence of the PAH shell layer, the appropriate distance between the fluorophore molecules and the Ag NPs is as beneficial to the fluorescence enhancement as the sample of PAH–Ag NPs.

It is generally known that the MEF effect is greatly sensitive to the interaction distance between the fluorophore and the metal NPs.[31,33] As a pH-responsive nanoparticle of PAH–Ag, the distance between the Ag NPs and the Por^{4+} adsorbed on the surface of the nanoparticles can be easily modulated with various pH values. Therefore, to further study the tunable MEF, the PAH–Ag NPs with different pH values were added into the Por^{4+} solution. After the Por^{4+} molecules were sufficiently adsorbed on the surface of the PAH–Ag NPs, the emission peak intensity at a wavelength of 653 nm was measured with the excitation wavelength at 420 nm. For comparison, the pure Por^{4+} solution with the same concentration was also measured as a reference. As shown in Fig. 7, the MEF efficiency decreased with the increase of the pH of the solution and the Por^{4+}/PAH–Ag NPs exhibited an MEF effect with 1.97-fold fluorescence enhancement at pH = 4. The reason is that the MEF effect is very sensitive to the different interaction distance between fluorophore and Ag NPs. For the PAH–Ag NPs, the shell thickness of the PAH–Ag NPs decreases at the lower pH, which suggests that the interaction distance between the fluorophore and Ag NPs can be tuned by adjusting the pH of the dispersion

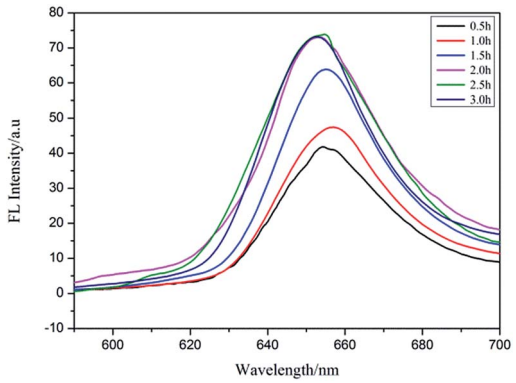

Fig. 5 Emission spectra of Por^{4+}/PAH–Ag dispersion at different incubation times.

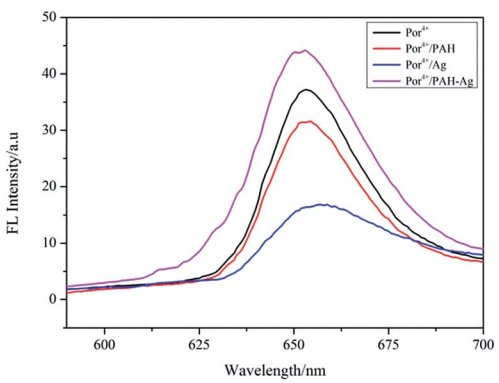

Fig. 6 Emission spectra of Por^{4+} solution, Por^{4+}/PAH dispersion, Por^{4+}/Ag dispersion and Por^{4+}/PAH–Ag dispersion at pH = 7.

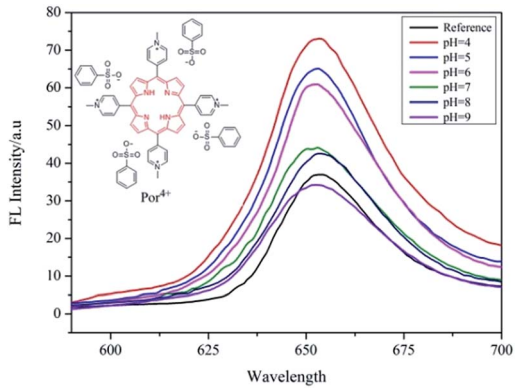

Fig. 7 Emission spectra of Por^{4+} solution at pH = 7 and Por^{4+}/PAH–Ag dispersion at different pH values.

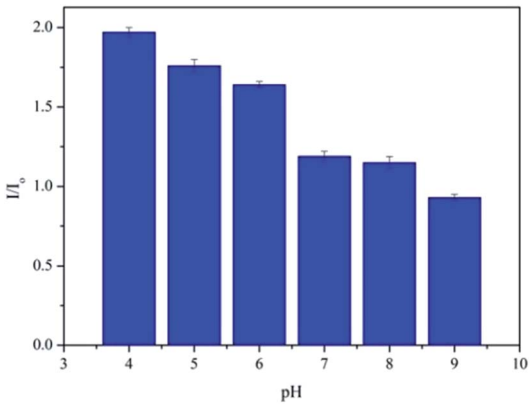

Fig. 8 Relative fluorescence enhancement factors of Por^{4+} by adding PAH–Ag NPs at different pH values.

solution. With the decrease of the distance between the fluorophore and Ag NPs, the influence of surface plasmon resonance on the fluorescence enhancement increases. When the pH of the Por^{4+}/PAH–Ag dispersion is 4, the thickness of the PAH shell is quite close to the optimum interaction distance for the MEF effects.[34] It can achieve a maximum multiple of fluorescence enhancement. To further clarify the controllable MEF behavior, the plots of fluorescence enhancement factors and different pH values are shown in Fig. 8. It is clearly shown that the responsive MEF behaviors are consistent with the pH-responsive swelling–shrinking properties of the PAH–Ag NPs. These results indicate that we found a simple and effective method to employ tunable MEF by introducing a pH-responsive shell onto the surface of Ag NPs.

Conclusions

In summary, we firstly reported on the controllable MEF in the presence of pH-responsive PAH–Ag NPs. The PAH–Ag NPs were prepared by directly reducing the Ag^+ to Ag in the PAH polymer. The PAH–Ag NPs can undergo swelling–shrinking behavior in response to pH stimuli, which can effectively tune the interaction distance between the Por^{4+} molecules and the Ag NPs, and consequently realize a controllable MEF effect. By this method, we successfully achieved an MEF effect by adjusting the pH of the Por^{4+}/PAH–Ag dispersion, and a fluorescence enhancement of 1.97-fold can be generated when the pH of the PAH–Ag dispersion is 4, as compared with the Por^{4+} solution without adding PAH–Ag NPs. The responsive MEF behavior is in good accordance with the swelling–shrinking properties of PAH–Ag NPs at different pH values. These results indicate a new strategy to realize a tunable MEF by introducing a pH-responsive PAH shell onto the surface of Ag NPs by adjusting the external stimuli.

Acknowledgements

This work was supported by the National Natural Science Foundation of China (No. 51203018, 21671037 and 51503033), the Doctoral Program of Higher Education in China (No. 20130075130002) and the Fundamental Research Funds for the Central Universities (No. 2232015D3-14).

References

1 J. Yin, Y. Hu and J. Yoon, *Chem. Soc. Rev.*, 2015, **44**, 4619–4644.
2 Y. Wang, Y. Huang, B. Li, L. Zhang, H. Song, H. Jiang and J. Gao, *RSC Adv.*, 2011, **1**, 1294–1300.
3 H. Huang, J. J. Lv, D. L. Zhou, N. Bao, Y. Xu, A. J. Wang and J. J. Feng, *RSC Adv.*, 2013, **3**, 21691–21696.
4 F. Wang, L. Zhou, C. Zhao, R. Wang, Q. Fei, S. Luo, Z. Guo, H. Tian and W. H. Zhu, *Chem. Sci.*, 2015, **6**, 2584–2589.
5 Y. Yang, C. Yin, F. Huo and J. Chao, *RSC Adv.*, 2013, **3**, 9637–9640.
6 P. G. Luo, F. Yang, S. T. Yang, S. K. Sonkar, L. Yang, J. J. Broglie, Y. Liu and Y. P. Sun, *RSC Adv.*, 2014, **4**, 10791–10807.
7 D. J. Litman, Z. Harel and E. F. Ullman, *Macromolecular fluorescent quencher particle in specific receptor assays*, *US Pat.*, 1982.
8 W. Chen, K. D. Long, H. Yu, Y. Tan, J. S. Choi, B. A. Harley and B. T. Cunningham, *Analyst*, 2014, **139**, 5954–5963.
9 X. Zheng, S. Meng, J. Chen, J. Wang, J. Xian, Y. Shao, X. Fu and D. Li, *J. Phys. Chem. C*, 2013, **117**, 21263–21273.
10 K. Sreenath, Z. Yuan, J. R. Allen, M. W. Davidson and L. Zhu, *Chem.–Eur. J.*, 2015, **21**, 867–874.
11 H. Li, M. Wang, C. Wang, W. Li, W. Qiang and D. Xu, *Anal. Chem.*, 2013, **85**, 4492–4499.
12 C. Li, Y. Zhu, X. Zhang, X. Yang and C. Li, *RSC Adv.*, 2012, **2**, 1765–1768.
13 A. M. Gabudean, M. Focsan and S. Astilean, *J. Phys. Chem. C*, 2012, **116**, 12240–12249.
14 S. Sarkar, B. Kanchibotla, J. D. Nelson, J. D. Edwards, J. Anderson, G. C. Tepper and S. Bandyopadhyay, *Nano Lett.*, 2015, **14**, 5973–5978.
15 H. Li, C. Y. Chen, X. Wei, W. Qiang, Z. Li, Q. Cheng and D. Xu, *Anal. Chem.*, 2012, **84**, 8656–8662.
16 J. Ju, E. Byeon, Y. A. Han and S. M. Kim, *Micro Nano Lett.*, 2013, **8**, 370–373.

17 F. Xie, J. Pang, A. Centeno, M. Ryan, J. Riley and N. Alford, *Nano Res.*, 2013, **6**, 496–510.
18 N. Ma, F. Tang, X. Wang, F. He and L. Li, *Macromol. Rapid Commun.*, 2011, **32**, 587–592.
19 M. Dong, T. Yu and D. Pappas, *Anal. Methods*, 2014, **6**, 1598–1602.
20 L. Tong, N. Ma, F. Tang, D. Qiu, Q. Cui and L. Li, *J. Mater. Chem.*, 2012, **22**, 8988–8993.
21 X. He, Z. H. Lin, Z. L. Zhao, R. H. He, M. Zhang and H. L. Fan, *J. Nano Res.*, 2015, **33**, 1–10.
22 J. Zhang, N. Ma, F. Tang, Q. Cui, F. He and L. Li, *ACS Appl. Mater. Interfaces*, 2012, **4**, 1747–1751.
23 H. Ma, A. Li, Y. Xu, W. Zhang and J. Liu, *Eur. Polym. J.*, 2015, **72**, 212–221.
24 Y. Bae, N. Nishiyama, S. Fukushima, H. Koyama, M. Yasuhiro and K. Kataoka, *Bioconjugate Chem.*, 2005, **16**, 122–130.
25 A. Kumar, S. K. Samal, R. Dash and U. Ojha, *J. Mater. Chem. B*, 2014, **2**, 7429–7439.
26 R. R. Ujjwal, M. P. Purohit, S. Patnaik and U. Ojha, *ACS Appl. Mater. Interfaces*, 2015, **7**, 509–512.
27 A. Kumar, R. R. Ujjwal, A. Mittal, A. Bansal and U. Ojha, *ACS Appl. Mater. Interfaces*, 2014, **6**, 1855–1865.
28 A. S. Badran, A. A. Abd-El-Hakim, A. B. Moustafa and M. A. A. El-Ghaffar, *J. Polym. Sci., Part A: Polym. Chem.*, 1988, **26**, 609–614.
29 X. W. Wei, G. X. Zhu, Y. J. Liu, Y. H. Ni, Y. Song and Z. Xu, *Chem. Mater.*, 2008, **20**, 6248–6253.
30 R. Krämer, *Angew. Chem., Int. Ed.*, 1998, **37**, 772–773.
31 F. Tang, N. Ma, L. Tong, F. He and L. Li, *Langmuir*, 2012, **28**, 883–888.
32 D. Cheng and Q. H. Xu, *Chem. Commun.*, 2006, **3**, 248–250.
33 F. Tang, N. Ma, X. Wang, F. He and L. Li, *J. Mater. Chem.*, 2011, **21**, 16943–16948.
34 O. G. Tovmachenko, C. Graf, A. Van Blaaderen and H. C. Gerritsen, *Adv. Mater.*, 2006, **18**, 91–95.